Signal Processing and Renewable Energy
June 2023, (pp. 1-15)
ISSN: 2588-7327
eISSN: 2588-7335

Local Characteristic Decomposition as a Novel Approach to Predict Sudden Cardiac Death in Congestive Heart Failure Patients

Ali Dorostghol[1], Adel Maghsoudpour[1*], Ali Ghaffari[2], Mansour Nikkhah-bahrami[1]

[1] Department of Mechanical Engineering, Science and Research Branch, Islamic Azad University, Tehran, Iran.
[2] Department of Mechanical Engineering, K. N. Toosi University of Technology, Tehran, Iran.

Received: 01-Aug-2022, Accepted: 01-Jan-2023.

Abstract

The current study uses heart rate variability (HRV) signal processing to investigate changes in the multifractal dimension in congestive heart failure (CHF) patients and predict sudden cardiac death (SCD). In this regard, HRV signals are first extracted, and their four sub-signals are determined using the Local Characteristic Decomposition (LCD) method. In the next step, using the Teager Energy method, the instant amplitudes of each sub-signal obtained in the previous step are calculated; thus, new signals are generated based on these instant amplitudes. Employing multifractal detrended fluctuation analysis (MF-DFA), the modified fractal dimensions of each new signal are then obtained. With the t-test method, appropriate features are selected and input into the support vector machine (SVM) classifier. By detecting subtle changes in HRV signals, this method can detect SCD in CHF patients. The results indicate that the proposed algorithm can distinguish the signals of SCD subjects with an accuracy of 84.76% 26 minutes before the event. In addition, after passing each 5-minute interval, the proposed method can update and determine how much time is left before SCD occurs.

Keywords: Heart Rate Variability, Sudden Cardiac Death, Multi Fractal Dimension, Congestive Heart Failure.

1. INTRODUCTION

Sudden cardiac deaths are usually caused by cardiac disorders. A SCD occurs if it takes one hour or less from the onset of the final clinical event (such as arrhythmia, chest pain, and lightheadedness) to the cardiac arrest [1,2]. Despite all efforts, there is no practical way to predict this event at the right time.

*Corresponding Authors Email: a.maghsoudpour@srbiau.ac.ir

SCD is not completely understood yet, but ventricular fibrillation (VF) has been implicated in 20% of cases [3]. VF occurs when the heart's electrical activity is disrupted, resulting in the heart's inability to provide and pump blood to vital organs. In the absence of proper clinical procedures, this will cause the patient's death. In the U.S., at least 300,000 people die from SCDs outside the hospital each year [4]. Identification of people at risk of SCD is therefore crucial for timely preparation and reducing the death rate.

In recent years, various researchers have studied SCD syndrome using ECG or HRV signal analysis. Most of them attempt to use features of the autonomic system that can help detect SCD, since SCD is accompanied by an autonomic disorder. For instance, by employing wavelet analysis and six features of Higuchi fractal dimension, Hurst exponent, approximation entropy, sample entropy, DFA, and correlation dimension, Acharya [5] were able to predict SCD with an accuracy of 86.8% four minutes before occurrence. In another study, by extracting the nonlinear features of the HRV signal from twenty patients and eighteen healthy subjects and applying the SVM algorithm, Fujita et al. predicted death chance with an accuracy of 94.7% four minutes before it occurred [6]. Another investigation conducted by Ebrahimzadeh et al. examined nine linear characteristics and could anticipate the event 13 minutes earlier than its happening [7]. They used four nonlinear characteristics, 11 characteristics within the time-frequency domain, and employed the techniques of selecting local characteristics at different times. The reported accuracy of the created multilayer perceptron network was 90.18%. Their Results show that chaotic events and time-frequency characteristics are amplified by increasing the duration of the prediction.

The complicated behavior of SCD prevents recruiting only normal people as comparison groups. Nonetheless, the earlier investigations have employed the ECG signals of normal people as comparison groups, which brings about a significant constraint. For instance, CHF patients suffer a higher rate of SCD in comparison with other people. As a result of insufficient energy, the heart cannot pump blood at regular heart pressures in the mentioned disease [8]. An approximate population of 26 million individuals suffers from the same illness around the world [9]. A great number of similarities are found between the cardiac signal characteristics of the patients suffering congestive heart failure and the cardiac signal characteristics of the individuals suffering SCD some hours before the occurrence. Therefore, by conducting a comparison between the two groups, one can determine the onset of the shifts in cardiac signals of the individuals suffering SCD and the cardiac step towards occurrence. In recent years, an algorithm was presented by Devi et al. in order to distinguish between HRV signals in subjects suffering from SCD and CHF patients and healthy subjects [10]. When 32 non-linear, classical, and CWT characteristics were used, 10 minutes earlier than the occurrence of VF, the reported accuracy of the created neural network was 83.33%. Rohila et al. separated the heart rate variability (HRV) signals of the subjects at risk of SCD from normal individuals and the patients suffering from CHF, SCD, and

coronary artery disease (CAD) an hour earlier than the event [11]. Nonetheless, in spite of promising results, the efficiency of their classification is slightly varied with the interval earlier than the VF event. As a result, their technique is not capable of detecting subtle changes in the heart rate variability signals. In fact, when it comes to the comparison of multiple groups, detecting changes in HRV signals becomes more difficult. Hence, in this study, the following two objectives are addressed: (1) Deciding the point in time in which signal shifts take place in the subjects at risk of SCD. (2) Anticipation of SCD in patients suffering from congestive heart failure on the basis of the signal shifts. This has been realized via the LCD technique, in which signals are decomposed into constituent sub-signals. In recent years, the LCD technique has been presented for the analysis of the vibration signals caused by gearbox bearings. According to the reports, this technique has fewer problems associated with mode mixing in comparison with the EMD technique [12,13,14].

2. MATERIALS AND METHODS

2.1. Data Base

The proposed algorithm is applied to the available signals in the MIT-BIH Sudden Cardiac Death Holter Database and Congestive Heart Failure RR Interval Database. MIT-BIH's database contains the cardiac signals of 23 subjects with SCD. From the 23 subjects whose information is available in the database, 20 subjects are diagnosed with VF, and the remaining three subjects do not present VF episodes. Consequently, three subjects are excluded from the investigation process. On the other hand, Congestive Heart Failure RR Interval Database also contains the RR signal of 29 patients [15]. The HRV signal of existing CHF patients often includes a regular rhythm and occasionally an abnormal rhythm (mostly premature ventricular contraction (PVC) and atrial fibrillation).

2.2. Preprocessing of Signals

A five-minute interval is initially isolated from the ECG signal of people with SCD syndrome from 61 minutes to 1 minute before the event. After denoising, the R-wave peaks are determined using the Pan-Tampkins algorithm; subsequently, the HRV signal is generated by assembling the RRs. (Because the RR signal of CHF patients is available in the mentioned database, generating this signal from the ECG is pointless). In the following, from the cardiac signals of CHF patients, 5-minute intervals are randomly selected. It should be noted that because of severe noise, RR intervals longer than 3 seconds have been removed from the calculations.

Figure 1 depicts two HRV signals extracted from mentioned databases.

2.3. Feature Extracting

The technique suggested for the prediction of SCD has been represented within a block diagram in Fig. 2. Every single five-minute segment of the heart rate variability signals will be decomposed into four sub-signals known as intrinsic scale components (ISC) in step 1. Then, in step 2, the Teager Energy Operator (TEO) technique is used in order to

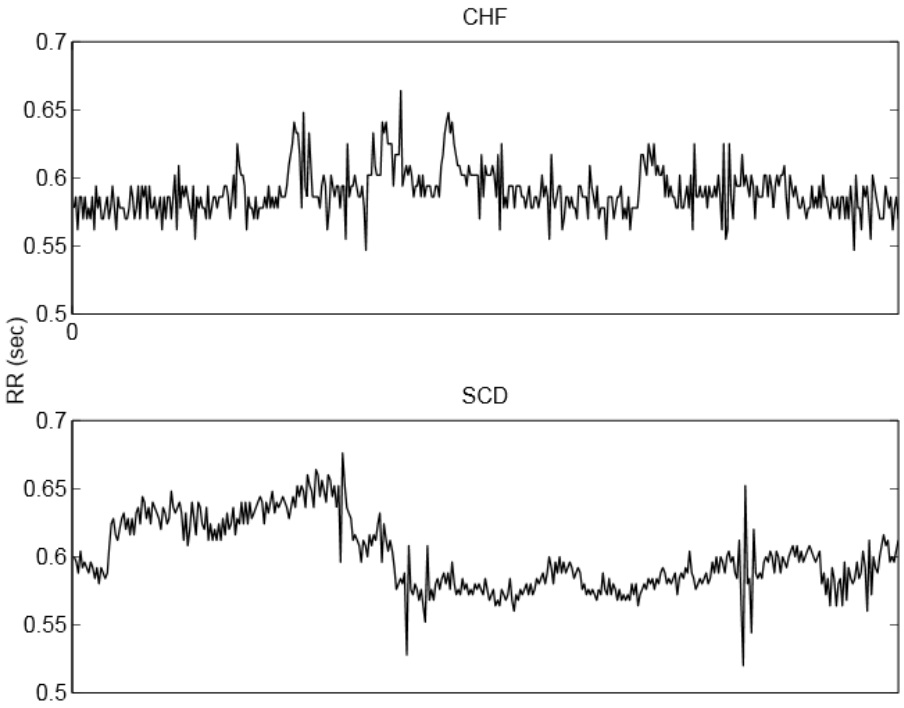

Fig. 1. HRV signals of two classes.

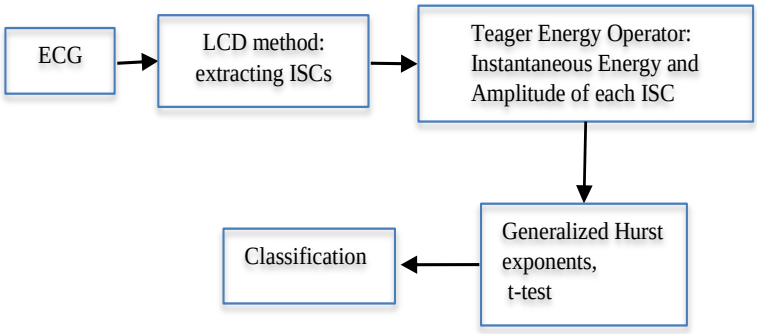

Fig. 2. The block diagram of the feature extraction and SCD prediction stages.

obtain the instant amplitude signal for every single intrinsic scale component. Finally, in order to analyze the multi-fractal features of each new signal in step 3, the technique of multi-fractal detrended analysis will be employed. Using the t-test method, the number of features (44 features) is reduced in step 4. In step 5, the selected features are applied to the SVM classifier as input data.

2.3.1. Local Characteristic Decomposition

LCD is a new signal processing technique used for non-stationary time series decomposition [12]. Like the empirical mode

decomposition (EMD) method, it decomposes a given signal *x(t)* into a set of sub-signals, called intrinsic scale components (*ISCs*). By the LCD procedure, K modes ($d_k(t)$) and a residual term *(r(t))* are extracted and communicated by relation (1).

$$x(t) = \sum_{k=1}^{n} d_k(t) + r(t) \qquad (1)$$

To extract the ISCs from an LCD algorithm, the following steps must be performed iteratively:

In step 1: Connect any two adjacent maxima (minima) by a straight line (Figure 3).

In step 2: By relation (2), the point corresponding to the minima (maxima) is determined according to Figure 2.

$$A_k = x_{k-1} + \frac{t_k - t_{k-1}}{t_{k+1} - t_{k-1}}(x_{k+1} - x_{k-1}) \qquad (2)$$

In step 3. From equation (3) we find (t_k, L_k), the point that lies in the middle of the straight line that connects (t_k, x_k) to (t_k, A_k).

$$L_k = aA_k + (1-a)x_k \qquad (3)$$

Here (a) is equal to 0.5.

In step 4. all the $L_k(k = 1, \dots, M)$ are connected with cubic spline interpolation (SL). This difference between the signal x(t) and $SL_1(t)$can be calculated using equation (4).

$$h_1(t) = x(t) - SL_1(t) \qquad (4)$$

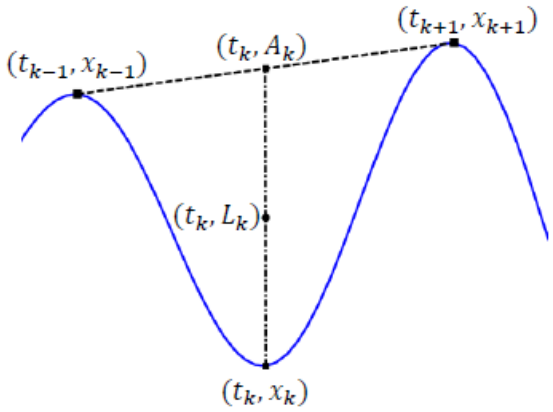

Fig. 3. Part of LCD algorithm [16].

In the entire data sets, all of the maximum local points are positive and all of the minimum local points are negative and the signal is monotonic between any two successive extreme points. The details of the LCD method are discussed in the reference [13].

The first ISC of x(t) is $h_1(t)$ if it meets the criteria of ISC.

In step 6. as long as $h_1(t)$ is not an ISC, it is taken as the original signal and the above steps are repeated until $h_m(t)$ is an ISC after m iterations. Here, standard deviation (SD) is a criterion used to stop iterations:

$$SD = \sum \left[\frac{|r_{n-1}(t) - r_n(t)|^2}{{r_{n-1}}^2(t)} \right] < threshold \qquad (5)$$

In step 7. The residue r_1 which is treated as the original signal is obtained from relation (6).

$$r_1 = x(t) - ISC_1 \qquad (6)$$

in which ISC_1 is the first *ISC*.

Table 1. ***Pseudo code of the LCD algorithm.***

1) Start
2) Input the original signal: X(t)
3) input the threshold (μ)
4) r=X(t)
5) n=1
6) Locate all the extrema of r: $(\boldsymbol{t_k}, \boldsymbol{x_k})$; k=1, …, m
7) for k=1, …, m calculate:

$$\boldsymbol{A_k} = \boldsymbol{x_{k-1}} + \frac{\boldsymbol{t_k}-\boldsymbol{t_{k-1}}}{\boldsymbol{t_{k+1}}-\boldsymbol{t_{k-1}}}(\boldsymbol{x_{k+1}} - \boldsymbol{x_{k-1}}) \ ,$$

$$\boldsymbol{L_k} = \boldsymbol{0.5}(\boldsymbol{A_k} + \boldsymbol{x_k})$$

end for
8) Use spline (SL) to connect all the $\boldsymbol{L_k}$
9) h=r-SL
10) while all of the maxima>0 and all of the minima<0
Repeat step 6 to 10
end while
11) $\boldsymbol{Isc_n} = \boldsymbol{h}, \boldsymbol{r} = \boldsymbol{r} - \boldsymbol{Isc_n}$
12) n=n+1
13) Calculate: $\boldsymbol{SD} = \left[\frac{|\boldsymbol{r_{n-1}}(t)-\boldsymbol{r_n}(t)|^2}{\boldsymbol{r_{n-1}}^2(t)}\right]$
14) while SD > μ and the number of extrema is more than 2
Go to step 6
end while
15) Print $ISC_{1...n}$
16) end

In step 8. The above procedure is repeated n times to yield n ISC and a residue. When the residue becomes monotonous, the procedure terminates.

It should be noted that High-order ISCs correspond to low frequency, while low-order ISCs correspond to high frequency. The pseudo-code of the LCD algorithm is displayed in Table 1.

2.3.2. Teager-Kaiser Energy Operator

The amplitude and frequency of the sub-signals obtained from the LCD method are unstable and time-variant. As a result, amplitude changes can be used to extract signal properties. Therefore, the Teager-Kaiser energy operator method is used to determine the frequency and local size of signals. In comparison to the Hilbert conversion method, this method is less computationally complex and more efficient in analyzing signals with shocks [17]. Due to the abilities mentioned above, the Teager-Kaiser method is employed in this study to determine the frequency and size of the obtained sub-signals.

For discrete signals, this operator is determined as follows:

$$\psi[x(n)] = x^2(n) - x(n-1) \times x(n+1) \quad (7)$$

$x(n)$ and $x(n+1)$ and $x(n-1)$ are all that are needed to calculate the value of the mentioned operator. Thus, it is very sensitive to change and has a very high resolution.

The instant frequency and amplitude of the signal are acquired from the subsequent equations:

$$F(n) = \frac{1}{4\pi f}\arccos\left(1 - \frac{\psi[x(n+1) - x(n-1)]}{2\psi[x(n)]}\right) \quad (8)$$

$$|A(n)| = \frac{2\psi[x(n)]}{\sqrt{\psi[x(n+1) - x(n-1)]}} \quad (9)$$

in which, f is the sampling frequency.

2.3.3. MF-DFA Method

The constituent five steps of the MF-DFA technique are as below [18]:

1- If x_k stands for a time series featuring the length of N, then:

$$Y(i) = \sum_{k=1}^{i} |x_k - \langle x \rangle|, \quad i = 1, \dots, n \tag{10}$$

In which:

$$\langle x \rangle = \frac{1}{N} \sum_{k=1}^{i} x_k \tag{11}$$

2- $Y(i)$ time series will be decomposed into *m* segments with no overlaps with the length of *s*, where *m* is determined from *m=int(N/s)*. In order to make optimal use of the whole data in a similar manner, the data will be also segmented into *m* parts from last to first. Therefore, a total of *2m* data series will be created, each featuring a length of *s*.

3- The least squares error relationship in every single segment determines the trend. $F^2(s, \vartheta)$ stands for the least squares error, which is determined via the equation below if $\vartheta = 1, \dots, m$:

$$F^2(s, \vartheta) = \frac{1}{s} \sum_{i=1}^{s} \{Y[(\vartheta - 1)s + i] - y_\vartheta(i)\}^2 \tag{12}$$

However, if $\vartheta = m = 1, \dots, 2m$

$$F^2(s, \vartheta) = \frac{1}{s} \sum_{i=1}^{s} \{Y[N - (\vartheta - m)s + i] - y_\vartheta(i)\}^2 \tag{13}$$

$y_\vartheta(i)$ in the above-cited relations stands for the polynomial fit (trend) of segment ϑ. One may consider this polynomial linear or with higher degrees. Evidently, the obtained results are dependent on the order of such a polynomial.

4- The fluctuation function of q order is decided by averaging in relation to the whole segments as below:

$$F_q(s) = \left\{ \frac{1}{2m} \sum_{\vartheta=1}^{2m} [F^2(s, \vartheta)]^{q/2} \right\}^{1/q} \tag{14}$$

Considering the fact that in the above equation, the expression 1 / q becomes infinite for q = 0, the equation must be redefined as:

$$F_q(s) = exp\left\{ 0.5 \times \frac{1}{2m} \sum_{\vartheta=1}^{2m} [\log (F^2(s, \vartheta)^2] \right\} \tag{15}$$

Given the various lengths of *s*, the $F_q(s)$ function is obtained by repeating steps 2-4, which is dependent on the variables *q* and *s*. The increased *s* obviously increases $F_q(s)$.

5- At every single order of various *s* and *q*, the relationship between *log* (*s*) and *log* ($F_q(s)$) is decided. If the future signal changes are dependent on the present signal changes, then the increased *s* leads to an exponential increase in $F_q(s)$:

2.4. Features Ranking

It must be kept in mind that not all the investigated features may be beneficial for differentiating between CHF patients and those with SCD. Two popular methods for reducing feature vectors' dimensions are linear discriminant analysis (LDA) and principal component analysis (PCA). Nonetheless, after the reduction of dimensions via the abovementioned techniques, one cannot interpret the features

appropriately. As a result of the mentioned technique, the t-test method is used in order to categorize and decide the effectiveness of every single feature in the present investigation. The t-test is used in order to find out the absence/presence of noticeable differences between the two data collections. After applying this test, the P-values are announced. In this regard, features with a P-value of less than 0.05 are selected to be exploited in the classification algorithm of this study.

2.5. Support Vector Machine classifier

An important aspect of the SVM algorithm is its ability to classify various data sets using hyperplanes [19,20]. This algorithm can classify data both linearly and nonlinearly. Radial basis functions (RBFs) and polynomial kernel functions are used in this study for classifying signals of patients. Since the signals of subjects who die suddenly within minutes are separated from the signals of other patients, this classification could be regarded as a prediction. Here, leave-one-out cross-validation is used to train the classifier.

The performance evaluators for predicting SCD were specificity, sensitivity, and accuracy. Equations 17 to 19 are applied to determine the mentioned measures.

$$SN = \frac{TP}{FN + TP} \quad (17)$$

$$SP = \frac{TN}{TN + FP} \quad (18)$$

$$ACC = \frac{TP + TN}{TN + TP + FN + FP} \quad (19)$$

where:

TP: The number of SCD subjects that are correctly detected as SCD.

TN: the number of CHF patients that are correctly detected as CHF.

FP: the number of patients with CHF misdiagnosed as having SCD.

FN: the number of SCDs misdiagnosed as CHF.

3. RESULTS AND DISCUSSIONS

3.1. Results

Following the LCD analysis of the signals (Figure 4), the TEO method determines the instant amplitude of the first four sub-signals. In the next step, the LCD-DFA method is applied to the signals resulted from the instant amplitudes. The first four intrinsic scale components obtained from the signals of congestive heart failure and the first SCD signal segment (1-6 minutes earlier before the event) have been presented in Fig. 5 for various values of q. The present investigation utilized an index scale (q) value ranging from -5 to 5. Such an interval includes the effects of large/small fluctuations in the instant amplitude signal when deciding the multifractal structure.

H(q) of the CHF and SCD signals at different time intervals. The stars shown in these tables are used for the purpose of marking the significant P-values. It is notable that we removed the segments featuring more than 30 seconds of noise. As a result, in a number of segments, instead of examining 20 subjects, fewer numbers were scrutinized.

Table 2. The P-Value obtained from comparing the results of the first segment of the SCD signal with the CHF signal. * indicates P<0.05.

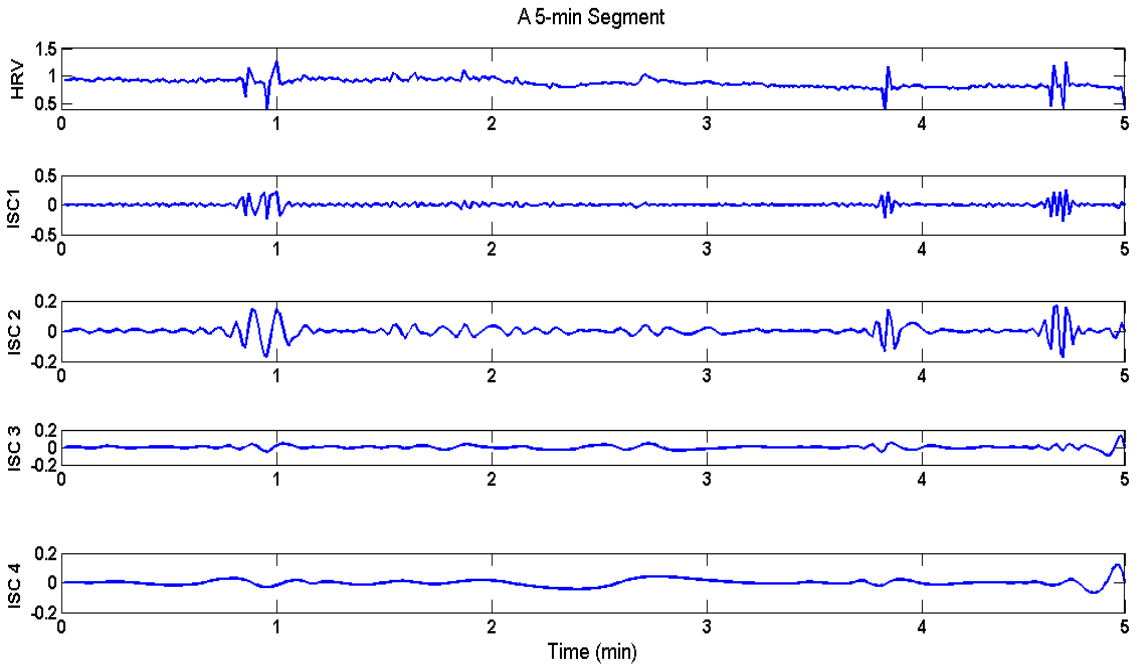

Fig. 4. The HRV signal and the four sub-signals obtained from the LCD method.

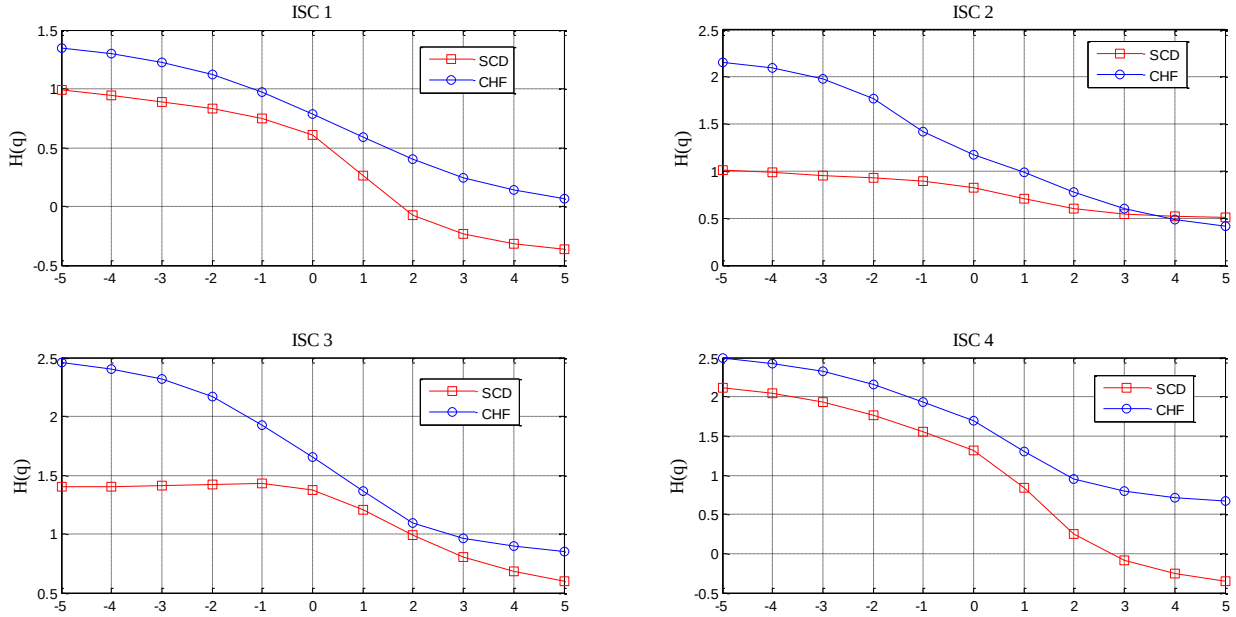

Fig. 5. Results obtained from four first ISCs of the CHF signals and the first SCD signal segment (1 to 6 minutes before the event).

Tables 2 to 6 represent the obtained P-value of the t-test in comparing the results of *H(q)* of the CHF and SCD signals at different time intervals. The stars shown in these tables are used for the purpose of marking the significant P-values. It is notable that we

removed the segments featuring more than 30 seconds of noise. As a result, in a number of segments, instead of examining 20 subjects, fewer numbers were scrutinized.

Table 2. ***The P-Value obtained from comparing the results of the first segment of the SCD signal with the CHF signal. * indicates P<0.05.***

1st segment and CHF P Value											
q	-5	-4	-3	-2	-1	0	1	2	3	4	5
ISC1	0.85	0.83	0.77	0.73	0.98	0.18	0.04*	0.013*	0.01*	0.008*	0.01*
ISC2	0.84	0.82	0.81	0.71	0.83	0.51	0.06	0.054	0.037*	0.031*	0.034*
ISC3	0.65	0.63	0.64	0.59	0.83	0.19	0.057	0.051	0.067	0.063	0.062
ISC4	0.37	0.30	0.31	0.4	0.42	0.14	0.0001*	0.0001*	0.0001*	0.0001*	0.0001*

Table 3. ***The P-Value obtained from comparing the results of the second segment of the SCD signal with the CHF signal. * indicates P<0.05.***

2st segment and CHF P Value											
q	-5	-4	-3	-2	-1	0	1	2	3	4	5
ISC1	0.005*	0.006*	0.007*	0.009*	0.006*	0.0009*	0.003*	0.03*	0.11	0.18	0.24
ISC2	0.22	0.23	0.252	0.325	0.45	0.267	0.042*	0.013*	0.012*	0.012*	0.013*
ISC3	0.84	0.83	0.82	0.78	0.69	0.22	0.12	0.31	0.356	0.398	0.368
ISC4	0.433	0.415	0.399	0.51	0.69	0.29	0.002*	0.0005*	0.0009*	0.001*	0.001*

Table 4. ***The P-Value obtained from comparing the results of the third segment of the SCD signal with the CHF signal. * indicates P<0.05.***

3st segment and CHF P Value											
q	-5	-4	-3	-2	-1	0	1	2	3	4	5
ISC1	0.921	0.956	0.916	0.902	0.723	0.254	0.068	0.088	0.185	0.169	0.188
ISC2	0.56	0.57	0.599	0.785	0.892	0.536	0.041*	0.012*	0.01*	0.01*	0.01*
ISC3	0.265	0.271	0.27	0.261	0.22	0.066	0.06	0.268	0.435	0.49	0.487
ISC4	0.387	0.396	0.458	0.563	0.974	0.477	0.044*	0.038*	0.042*	0.043*	0.04*

Table 5. ***The P-Value obtained from comparing the results of the fourth segment of SCD signal with CHF signal. * indicates P<0.05.***

4st segment and CHF P Value											
q	-5	-4	-3	-2	-1	0	1	2	3	4	5
ISC1	0.61	0.63	0.671	0.705	0.734	0.698	0.398	0.285	0.272	0.259	0.203
ISC2	0.521	0.533	0.567	0.582	0.671	0.698	0.22	0.174	0.186	0.231	0.224
ISC3	0.401	0.415	0.432	0.487	0.762	0.298	0.34 1	0.952	0.842	0.808	0.792
ISC4	0.984	0.952	0.933	0.92	0.764	0.247	0.035*	0.022*	0.025*	0.023*	0.025*

Table 6. ***The P-Value obtained from comparing the results of the fifth segment of the SCD signal with the CHF signal. * indicates P<0.05.***

5st segment and CHF P Value											
q	-5	-4	-3	-2	-1	0	1	2	3	4	5
ISC1	0.733	0.788	0.895	0.947	0.992	0.408	0.432	0.212	0.225	0.22	0.224
ISC2	0.202	0.218	0.236	0.363	0.725	0.888	0.298	0.23	0.236	0.275	0.268
ISC3	0.101	0.163	0.192	0.215	0.298	0.258	0.542	0.785	0.634	0.583	0.598
ISC4	0.865	0.827	0.784	0.662	0.373	0.044*	0.008*	0.012*	0.014*	0.017*	0.017*

Table 7. ***Results obtained from classification algorithm.***

Time pre SCD (min)	No of SCD cases	TP	TN	FP	FN	ACC	SEN	SPE
6 to 1	20	20	28	1	0	97.9 %	100 %	96.5 %
11 to 6	20	18	26	3	2	89.8%	90 %	89.6%
16 to 11	20	17	23	6	3	81.6%	85 %	79.3%
21 to 16	20	16	23	6	4	79.5%	80%	79.3%
26 to 21	19	12	24	5	7	75%	63.1%	82.7%

The tables show that the size of P-values varies in different time segments before the event. Here, SVM classification is performed using the q size of arrays with a P value less than 0.05 in each time segment. The results of the SVM classification method are shown in Table 7. The highest accuracy can be observed in the first segment before the event. In the minutes leading up to the event, the HRV signal changed dramatically. Also, the model exhibits desirable sensitivity, specificity, and accuracy in the 4th segment

(21 to 16 minutes earlier than the event). On the other hand, the sensitivity of the network declines to 63.1% in the 5th segment before the event.

3.2. Discussion

As reported in Table 7, the longer the time before VF occurs, the more difficult it is to distinguish the signals from each other, so no noticeable difference can be found between the properties acquired from SCD 26 minutes before the event. As a result, it seems that multifractal changes in heart rate variability signals resulting in SCD begin 26 minutes before the event approximately. The average sensitivity, specificity, and accuracy for the mentioned 26 minutes are 83.62%, 85.48%, and 84.76%, respectively. Such a prediction interval provides the treatment personnel with enough time to carry out the necessary medical practices.

Table 8 compares the results of the proposed approach with some comparable studies. In a number of aspects, the results of the suggested classification surpass those of other mentioned investigations. For example, with the exception of segments 5 and 4, the present investigation employs different characteristics in distinct time segments. Therefore, our technique is capable of estimating the time remaining before the onset of SCD, which is considered one of the main benefits of our technique. It is evident that the event time of SCD is vital in the management of the tasks related to the transportation of patients to the healthcare facilities as well as the required clinical interventions. It is evident that prioritization of patients in some emergency conditions is necessary. For example, in the case that according to the diagnoses of the designed neural networks, at least two individuals would be at risk for SCD simultaneously, while only a limited number of emergency clinical facilities are available for their revival, prioritization of those patients is vital. Even though neural networks are capable of diagnosing SCD, they currently cannot determine the remaining time before the SCD occurrence following such a primary notification. The algorithm introduced in the present study can accurately predict the remaining time before occurrence due to the fact that it utilizes the existing features at different times in different sub-signals. Hence, the most important innovation of our study is the capability of the introduced method in determining the accurate time of the occurrence in every time interval before SCD. In this method, every 5 minutes remaining before the occurrence are updated following the initial notification of SCD risk.

Furthermore, in many of the studies presented, the comparison was between MIT/BIH SCD and Physiobank NSR database. We stated earlier that patients constitute a great number of the victims of SCD. A great number of the risk markers utilized in the cited investigations differ between normal subjects and cardiac patients without the SCD diagnosis. Therefore, it is necessary to conduct more studies on the anticipation of SCD in patients. As far as we know, only two investigations, i.e., Rohila's study, and Devi's investigation, have made a comparison between the cardiac patients and the SCD subjects. Devi and colleagues have presented an algorithm for the purpose of distinguishing SCD patients from healthy

subjects and those with CHF ten minutes earlier than the onset of VF with an accuracy of 83.33%. In contrast, our proposed algorithm's average accuracy in 11min before the event is 93.85%, which is better than the former study's performance. Using 1 hour ECG signal recordings, Rohila et al. reported an accuracy of 91.67%. The long duration of the signal reduces the resolution of prediction. Contrary to what was mentioned before, our method is able to detect subtle changes in ECG and, the accuracy of the prediction varies within the 5 minutes preceding the event. More than all these, ECG signals are complex in nature and are affected by many factors. Accordingly, comparing several groups decreases the ability to detect the onset time of subtle changes in the HRV signals.

Table 9 displays the mean frequency and standard deviation of the instantaneous frequencies of each ISC. It is evident that the first intrinsic scale component features an extra high-frequency band (0.4 - 1 HZ). The second intrinsic scale component features a high-frequency band (0.15-0.4 HZ), the third intrinsic scale component features a low-frequency band (0.04-0.15 HZ), and the fourth intrinsic scale component features an additional low-frequency band (0.003-0.04 HZ). This table proves the superiority of LCD through HRV decomposition. LCD shows a good performance in dealing with the physiological signals compared to traditional linear methods, which causes an inaccurate decomposition of HRV.

Table 6 illustrates how altered signals are initially observed in people with SCD in ISC4. The physiological mechanism of this band is yet to be discovered, but it is most likely influenced by the renin-angiotensin-aldosterone system and the body's

Table 8. ***Comparison of the results of the proposed method with some previous studies.***

Author	Compared classes	Time and Accuracy
Fujita, et al	18 normal, 23 SCD	4 min before: 94.7%
Ebrahimzadeh, et al	35 normal, 35 SCD	13 min before: averagely 90.18%
Devi, et al	18 normal, 23 SCD, 15 CHF	10 min before: 83.33%
Rohila, et al	18 normal, 20 SCD, 15 CHF, 23 CAD	60 min before: averagely 91.67%
Proposed method	20 SCD, 29 CHF	Averaged over 26 min before: 84.76%

Table 9. ***Frequency parameters of IMFs.***

Symbol	Mean IF±SD	Frequency Band
ISC1	0.42 ± 0.028	VHF
ISC2	0.179 ± 0.055	HF
ISC3	0.085 ± 0.0122	LF
ISC4	0.0241 ± 0.012	VLF

temperature regulation mechanisms [21]. In addition, multifractal changes take place for the scale indices ranging from 1 to 5. For positive q's, the fluctuation function is affected by the periods featuring large values of root mean squares. As a result, in the heart rate variability of the patients with SCD, the large variations occurring in the same segment are decreased. As time passes and by inspection of the moments in the vicinity of the time of the event, other sub-signals, e.g., ISC1 and ISC2, exhibit more changes.

4. CONCLUSION

In the case of nonlinear signals, such as HRV signals, LCD is a reliable method. This study presents a method for predicting SCD by separating SCD from CHF patients. Initially, the LCD technique is used to decompose the heart rate variability signals of the patients suffering from CHF and SCD into four sub-signals (ISCs). Once the instant amplitude of each ISC is determined using the TEO method, the MF-DFA method reveals the multifractal properties of those signals. Based on our findings, the onset time of dynamic changes in HRV signal fractal dimensions is around 26 minutes before the event. These changes occur in the SCD signal from ISC4, which has a very low frequency. In a larger number of ISCs, changes are gradually observed as the event draws near. Using the selected features, the proposed methodology shows an average accuracy of 84.76 percent 26 minutes before the event. Consequently, LCD is an effective method of investigating HRV signals and distinguishing CHF patients from SCD subjects.

REFERENCES

[1] H. J. J. Wellens, P. J. Schwartz, F. W. Lindemans, A. E. Buxton, et al, Risk stratification for sudden cardiac death: current status and challenges for the future, Eur Heart J. Vol. 35, No. 25, pp. 1642–51, July 2014.

[2] G. I. Fishman, S. S. Chugh, D. Marco, et al, Sudden cardiac death prediction and prevention Circulation. Vol. 122, No. 22, pp. 2335-2348, November 2010.

[3] N. J. Pagidipati, T. A. Gaziano, Estimating deaths from cardiovascular disease: A review of global methodologies of mortality measurement Circulation. Vol. 127, No. 6, pp. 749-756, February 2013.

[4] P. Markwerth, T. Bajanowski, I. Tzimas, *et al.*, Sudden cardiac death—update. Int J Legal Med. Vol. 135, pp. 483–495, December 2021.

[5] U. R. Acharya, H. Fujita, V. K. Sudarshan, et al, An integrated index for detection of sudden cardiac death using discrete wavelet transform and nonlinear features. Knowl Based Syst. Vol. 83, pp. 149-158, March 2015.

[6] H. Fujita, U. R. Acharya, V. K. Sudarshan, et al, Sudden cardiac death (SCD) prediction based on nonlinear heart rate variability features and SCD index. Appl Soft Comput. Vol. 43, pp. 510-519, March 2016.

[7] E. Ebrahimzadeh, A. Foroutan, M. Shams, et al, An optimal strategy for prediction of sudden cardiac death through a pioneering feature-selection approach from HRV signal. Comput Methods Programs Biomed. 169:19-36,

February 2019.

[8] A. A. Bhurane, M. Sharma, R. San-Tanc, U. R. Acharya, An efficient detection of congestive heart failure using frequency localized filter banks for the diagnosis with ECG signals, Cog. Syst Res. Vol. 55, pp. 82-94, June 2019.

[9] M. Kumar, R. B. Pachori, U. R. Acharya, Use of accumulated entropies for automated detection of congestive heart failure in flexible analytic wavelet transform framework based on short-term HRV signals, Entropy. Vol. 19, No. 3:92, pp. 01-2, February 2017.

[10] R. Devi R, H. K. Tyagi, D. Kumar, A novel multi-class approach for early-stage prediction of sudden cardiac death. Biocybern. Biomed Eng. Vol. 39, No. 3, pp. 586-598, June 2019.

[11] A. Rohila, A. Sharma, Detection of sudden cardiac death by a comparative study of heart rate variability in normal and abnormal heart conditions, Biocybern Biomed Eng. Vol. 40, No. 3, pp. 1140-1154, June 2020.

[12] J. Zheng, J. Cheng, Y. Yang, A rolling bearing fault diagnosis approach based on LCD and fuzzy entropy, Mech Mach Theory. Vol. 70, No. 6, pp. 441, December 2013.

[13] H. Liu, X. Wang, C. Lu, Rolling bearing fault diagnosis based on LCD–TEO and multifractal detrended fluctuation analysis, Mech Syst Signal Process. Vol. 273, pp. 60-61, August 2015.

[14] L. Wang, Z. Liu, An improved local characteristic -scale decomposition to restrict end effects, mode mixing and its application to extract incipient bearing fault signal, Mech Syst Signal Process, Vol. 156, No. 10, July 2021.

[15] A. L. Goldberger, L. A. Amaral, L. Glass, et al, Physiobank, physiotoolkit, and physionet. Circulation. Vol. 101, No. 23, pp. e215–20, Jun 2000.

[16] A. Dorostghol, A. Maghsoudpour, A. Ghaffari, M. Nikkhah-Bahrami, Power line interference and baseline wander removal from ECG signals using local characteristic decomposition, Jinst. Vol. 17, June 2022.

[17] A. O. Boudraa, F. Salzenstein, Teager–Kaiser energy methods for signal and image analysis: A review, Digital Sig Proc. Vol. 78, pp. 338–375, March 2018.

[18] P. Shang, Y. Lu, S. Kamae, Detecting long-range correlations of traffic time series with multifractal detrended fluctuation analysis, Chaos Solitons Fractal. Vol. 36, No. 1, pp. 82-90, April 2008.

[19] D. Ro, P. Eh, D. Gs, Pattern classification, 2nd Edition, Wiley-interscience, November 2012.

[20] S. Kotsiantis, Supervised machine learning: a review of classification techniques. Informatica. Vol. 31, pp. 249-68, January 2007.

[21] A. E. Draghici, J. A. Taylor, The physiological basis and measurement of heart rate variability in humans, J Physiol Anthropol. Vol. 35, No. 1, 22-35, September 2016.